The Flow of a Thin Liquid Film Past a Cylinder

M. Sellier[*,1]
[1]Fraunhofer-Institut für Techno- und Wirtschaftsmathematik (ITWM)
*Fraunhofer Platz 1, D-67663 Kaiserslautern, Germany, mathieu.sellier@itwm.fhg.de
(mathieu.sellier@canterbury.ac.nz from 01/11/2006)

Abstract: This paper presents a numerical study of the flow of a thin liquid film past a circular cylinder. It is investigated in the framework of the lubrication approximation and the corresponding governing equations, formulated in a weak form, are solved in the FEMLAB environment. The effect of the diameter of the circular cylinder on the shape of the free surface is explored and potentially useful correlations derived.

Keywords: thin liquid films, solid inclusion, FEMLAB.

1. Problem description and solution strategy

The flow of a thin liquid film appears in many branches of science and industry, applications including, for example, the deposition of coatings and inks, direct patterning of functional layer during microchip production, spreading of pesticide or, the flow of oil in heat exchangers. The effect of solid bodies on the flow has been studied in many different contexts but never, to the best of the author's knowledge, in the one of thin liquid films. The civil engineering equivalent of this problem is the flow of a river past a bridge pillar, [1]. The aim of this study is to present a detailed numerical investigation of the flow of a thin liquid film down an inclined plane past a circular cylinder and, more specifically, to explore the effect of the cylinder diameter on the film free surface.

The liquid considered is Newtonian with viscosity μ and surface tension σ. Figure 1 illustrates the problem under consideration, the adopted notations and the boundary conditions. The film is fed by a constant volumetric flow rate Q_0 and flows down a square substrate inclined at an angle α to the horizontal. It meets a solid cylinder of diameter D, centered at (x_0,y_0) and, the substrate extends over $L=10D$ in both directions.

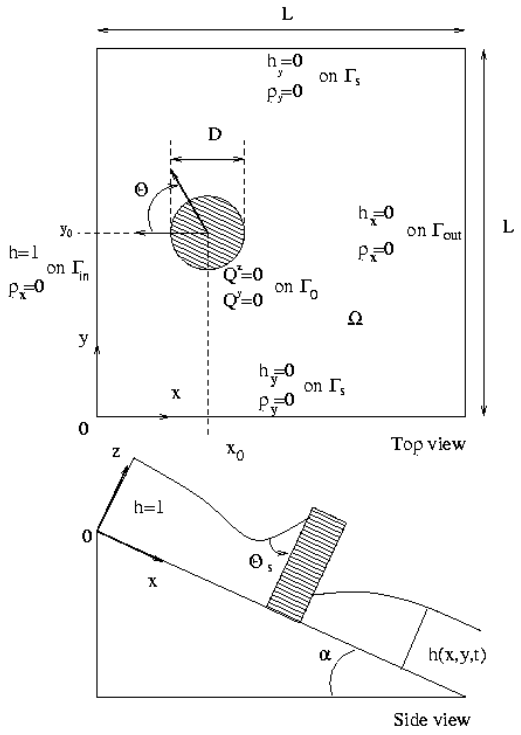

Figure 1: Top and side views of the flow of a thin liquid film down an inclined plane around a circular cylinder. The subscript indicates partial differentiation.

The flow is analyzed in the usual lubrication approximation framework and, following [2], for example, the equations governing the dimensionless film thickness $h(x,y,t)$ and pressure $p(x,y,t)$ averaged across the thickness read,

$$\frac{\partial h}{\partial t}+\nabla\cdot\underline{Q}=0\,, \qquad (1)$$

$$p+6\nabla^2 h=0\,, \qquad (2)$$

In $\Omega=[0,L]\times[0,L]\backslash\Omega_0$ where $\nabla=(\frac{\partial}{\partial x},\frac{\partial}{\partial y})$ and Ω_0 is the footprint of the cylinder on the substrate. Assuming a parabolic velocity profile,

the flux vector $\underline{Q}$ defined as $(Q^x, Q^y) = \int_0^h (u^x, u^y)\, dz$ is given by:

$$\underline{Q} = -\frac{h^3}{3}\left(\nabla p - 2\mathbf{i}\right). \quad (3)$$

This nonlinear system of equations is often combined to yield a fourth order partial differential equation in term of the film thickness only. The film thickness is scaled with that of the fully developed flow $H_0 = \left(\frac{3\mu Q_0}{\rho g \sin\alpha}\right)^{1/3}$, the substrate coordinates *(x,y)* with the dynamic Capillary length $L_d = \left(\frac{\sigma H_0}{3\rho g \sin\alpha}\right)^{1/3}$ and, the pressure with $P_0 = \frac{\rho g L_d \sin\alpha}{2}$. This formulation neglects the effect of the normal component of the gravity and offers the advantage of being parameter free giving the following results a universal nature in the validity limits of the lubrication approximation.

The governing equations are completed with the boundary conditions reported in Figure 1. At the upstream boundary Γ_{in}, the flow is assumed to be fully developed ($h=1$ and $dp/dx=0$) and the gradients of h and p are imposed to vanish on the other outer boundaries of the domain Γ_s and Γ_{out}. Along the cylinder surface Γ_0, the no-flux constraint must be complemented by an additional condition to obtain a well-posed problem. The latter results from the fact that the contact line at the junction between the solid cylinder, the liquid film and the air must form a prescribed angle Θ_s (see Figure 1). This angle is referred to the static contact angle and is a quantitative measure of the wetting property of the solid by the liquid, [3]. Consequently, the condition $\nabla h \cdot \boldsymbol{n} = \tan\left(\frac{\pi}{2} - \Theta_s\right)$ is imposed at the cylinder surface.

Based on the work of References [4, 5] which proved that the flow of a thin liquid film past a submerged topography is stable for realistic values of the governing parameters, one can expect the existence of a steady-state solution to this problem. However, to ease the computations which are prone to divergence because of the nonlinearity of the governing equations, the long-time steady solution of the corresponding transient problem is sought.

Because of the curved boundary at the cylinder surface and the nature of the boundary condition there, the problem is best treated in the finite element setting. To this end, the governing equations are first formulated in the weak form by multiplying eqs. (1), (2) by the test functions u and v, respectively, integrating over the domain Ω and applying the Green's formula. The weak form finally reads,

$$\int_\Omega \left[u\frac{\partial h}{\partial t} + \nabla u.\left(\frac{h^3}{3}\left(\nabla p - 2\mathbf{i}\right)\right)\right] d\omega - \int_{\Gamma_{out}} u\frac{-2h^3}{3}\, d\gamma = 0,$$

$$\int_\Omega \left[vp - 6\nabla v.\nabla h\right] d\omega + \int_{\Gamma_0} 6v\tan\left(\frac{\pi}{2} - \Theta_s\right) d\gamma = 0.$$

The possibility to implement directly the weak form of Partial Differential Equations in the commercial finite element package FEMLAB, [6], is exploited to solve eqs. (4) and (5) with triangular Lagrange elements of order two on a mesh sufficiently fine to guarantee the mesh independency of the results (~ 5000 elements). The cylinder, centered at $(x_0,y_0)=(0.3L,0.5L)$, is located far enough from the domain boundaries so that these do not affect the flow field. Finally, since the size of the domain $L=10D$ is chosen to be proportional to the size of the cylinder, the computational domains for two different values of the diameter are homothetic guaranteeing truly comparable results with identical meshes.

2. Numerical results

Results are computed for cylinder diameters ranging from 1 to 8 dynamic Capillary lengths and a static contact angle equal to π/2, i.e. the fluid free surface meets the cylinder at a right angle. Below this range, the free surface variations become negligible and above, the strong thinning at the downstream end of the cylinder induces a large curvature of the free surface likely to invalidate the assumption of the lubrication approximation.

Figure 2 shows a three-dimensional view of the film free surface and the contours of film thickness for the steady-state flow past a cylinder with a 2.5 L_d diameter. The characteristic "horse-shoe" wave which forms at the free surface in the wake of the cylinder is reminiscent of the flow past submerged topographies, see [2,7,8] for example. The same flow rate argument given in [2] can be used here to describe the free surface

features. The fluid hits the upstream wall of the cylinder which induces a rise in the film thickness and the fluid is shed further downstream in the spanwise direction away from the blockage. This creates a mass loss immediately downstream of the blockage and therefore a decrease in film thickness. This interpretation is confirmed by the streamline plot in Figure 3. An important difference with the submerged topography case is the amplitude of the film thickness variation which is much larger here and can lead to the rupture of the film immediately downstream of the blockage.

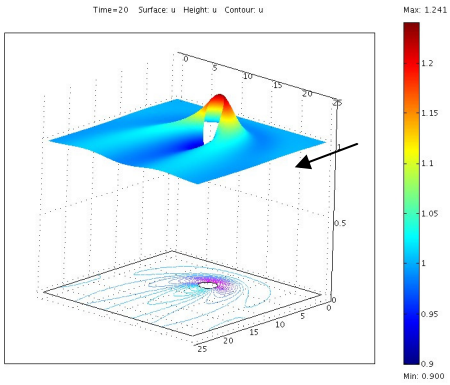

Figure 2: Three-dimensional view of the film free surface and corresponding contours for a 2.5 L_d cylinder diameter. The arrow indicates the direction of the flow.

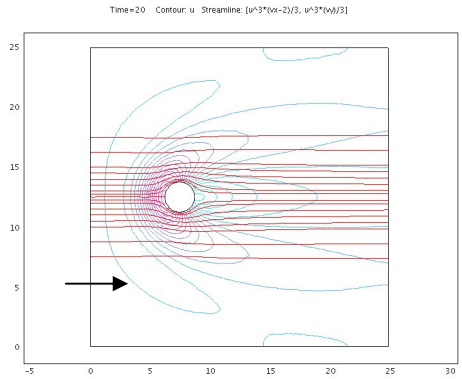

Figure 3: Streamlines based on the flux vector field (eq. (3)) and contours of film thickness for a 2.5 L_d cylinder diameter. The arrow indicates the direction of the flow.

The film thickness at the upstream ($\Theta=0$) and downstream ($\Theta=\pi$) ends of the cylinder is reported in Figure 4 as a function of the cylinder diameter. Two variation regimes, delimited by a diameter of approximately 1.75 L_d, are visible in this figure. The fitted lines indicate that the variation is linear in both regimes for the film thickness at the upstream and downstream ends. At the upstream end, the film thickness increases almost three times faster in the lower diameter range than in the higher one. At the downstream end, the film thickness remains initially constant, and then it decreases twice faster than it increases at the upstream one. Since $h=\alpha D+\beta$ according to the linear fits in Figure 4, the dimensional film thickness $\tilde{h}$ depends linearly on the dimensional cylinder diameter $\tilde{D}$ according to $\tilde{h}=\alpha\frac{H_0}{L_d}\tilde{D}+H_0\beta$. Using the previously defined length scales, the aspect ratio H_0/L_d is equal to $3^{1/3}\left(\frac{9\mu^2\rho g\sin\alpha}{\sigma^3}\right)^{1/9}Q_0^{2/9}$. Thus, for a given fluid and substrate inclination angle, the effect of the cylinder diameter on the free surface variations is greater for larger flow rates.

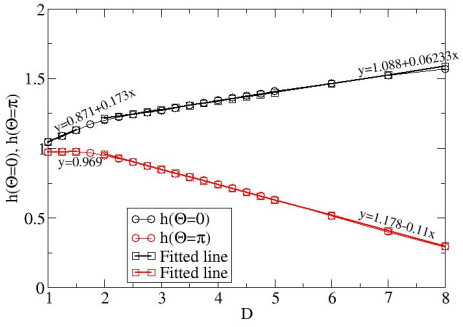

Figure 4: Film thickness at the upstream and downstream ends of the cylinder as a function of the cylinder diameter with the fitted lines and corresponding equations.

Figure 5 shows the resultant force exerted on the cylinder, computed according to

$$F=\int_{\Gamma_0} hpd\gamma=\frac{D}{2}\int_0^{2\pi} hpd\Theta. \qquad (4)$$

Remarkably, the data are perfectly fitted by the parabola $y=1.5068+1.3288x+0.3516x^2$ shown in the Figure and the value at the origin is noticeably close to $\pi/2$, a hint that an analytical treatment of the problem may be possible.

Finally, Figure 6 plots the film thickness along the cylinder for several values of the cylinder diameter. The figure shows that the transition angle along the cylinder where the film thickness decreases from a value greater than one (the fully developed film thickness) to a value that is smaller appears to be almost constant and around 135°.

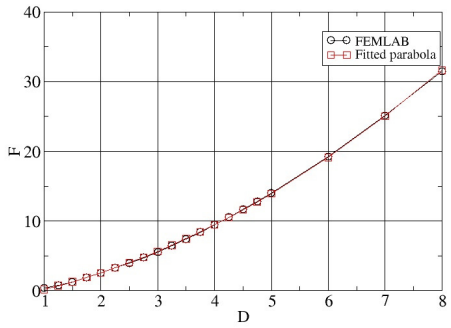

Figure 5: Resultant force exerted on the cylinder with the fitted parabola.

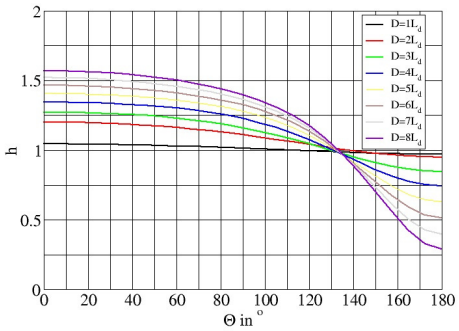

Figure 6: Film thickness profile along the surface of the cylinder for several diameters.

3. Concluding remarks

Despite the industrial applications and the scientific interest, the flow of a thin liquid film past a circular cylinder appears to be an unexplored problem. The present study attempts to partially fill this gap. The flow is investigated numerically in the lubrication approximation framework. Because of the curved boundary at the cylinder and the nonlinear flux condition there, the problem is best treated in the finite element framework. The governing equations are first reformulated in the weak form and then implemented and solved in the FEMLAB environment. Several remarkable trends have been outlined concerning, the film thickness at the upstream and downstream ends of the cylinder and the resultant force. These findings will be complemented in the future by an experimental investigation to assess the validity of the derived correlation.

4. References

1. Roulund A, Sumer BM, Fredsoe J and Mechelsen J, Numerical and experimental investigation of the flow and scour around a circular pile, *J. Fluid Mech.*, **534**, 351-401 (2005)
2. Gaskell PH, Jimack PK, Sellier M and Thompson HM, Gravity-driven flow of continuous thin liquid films on non-porous substrates with topography, *J. Fluid Mech.*, **509**, 253-280 (2004)
3. de Gennes PG, Wetting: statics and dynamics, *Rev. Mod. Phys.*, **57**, 827-863 (1985)
4. Kalliadasis S and Homsy GM, Stability of free-surface thin-film flows over topography, *J. Fluid Mech.*, **448**, 387-410 (2001)
5. Davis JM and Troian SM, Generalized linear stability of non inertial coating flows over topographical features, *Phys. Fluids*, **17**, art. no 072103 (2005)
6. Comsol, http://www.femlab.com
7. Hayes M, O'Brien SBG and Lammers JH, Green's function of steady flow over a two-dimensional topography, *Phys. Fluids*, **12**, 2845-2858 (2000)
8. Decré MMJ and Baret J-C, Gravity-driven flows of viscous liquids over two-dimensional topographies, *J. Fluid Mech.*, **487**, 147-166 (2003)